The effect of firing protocols on the resin-bond strength to alumina-coated zirconia ceramics

Tine Malgaj[a], *Andraž Kocjan*[b], *Peter Jevnikar*[a,] *

[a] Department of Prosthodontics, Faculty of Medicine, University of Ljubljana, Hrvatski trg 6, Ljubljana, Slovenia

[b] Department for Nanostructured Materials, Jožef Stefan Institute, Jamova 39, Ljubljana, Slovenia

* Corresponding author: peter.jevnikar@mf.uni-lj.si

Tel.: + 386 1 522 42 42

Declarations of interest: none

ABSTRACT

Bonding surface pre-treatment of zirconia ceramic dental restorations with a nanostructured alumina coating (NAC) provides a substantially stronger and durable bond than clinically established air-particle abrasion. However, the synthesis of NAC should completely comply with everyday dental laboratory practices. In the present study, the effect of various dental laboratory firing procedures, such as glaze, veneer and regeneration firings of zirconia, on the temperature-dependent phase evolution of NAC was studied (XRD) and related to the resin-cement shear-bond strength of as-sintered, high-pressure (4 bar) and low-pressure (1 bar) air-particle-abraded zirconia surfaces with or without a combination of MDP primer. Half of each sample groups (n=20) were subjected to 12000x thermocycles in water. The results were statistically analyzed using T-test and one-way ANOVA. When fired at 900 and 1050°C and topotactically transformed to γ- or a mixture of δ- and θ-aluminas, NAC provided highest and clinically acceptable bond-strengths (>20Mpa) not affected by thermocycling.

Keywords: *Zirconia ceramics; shear bond strength; nanostructured alumina coating; laboratory firing protocols*

1. Introduction

Yttria-partially-stabilised tetragonal zirconia (Y-TZP) ceramics offers a broad application in contemporary dentistry due to its biocompatibility, pleasing aesthetics and exceptional mechanical properties, such as high flexural strength and fracture toughness, as compared to other dental ceramics (1).

In order to achieve a long-term clinical success of the restoration, especially in the case of occlusal veneers, partial coverage restorations or resin-bonded fixed dental prostheses where mechanical retention is often limited due to a reduced bonding surface, a strong and durable bond between the ceramics and adhesive cement system is of utmost importance (2). It relies on micromechanical interlocking and chemical bonding. Therefore, the intaglio surface of the restoration needs to be pretreated before cementation (3, 4). Pretreatment protocols used to improve bonding characteristics of glass-ceramics such as hydrofluoric (HF) acid cannot be implemented for etching of sintered Y-TZP ceramics, due to its increased chemical stability and the inexistence of vitreous phase, which are impervious to etching with HF (3, 5).

To improve micromechanical interlocking and to increase the cementation surface area of Y-TZP restoration, airborne particle abrasion (APA), followed by the application of a primer containing adhesive monomer, which promotes chemical bonds to oxide-ceramics, has commonly been advocated (6, 7). It has been shown that APA in combination with an adhesive monomer, such as 10-Methacryloyloxydecyl dihydrogen phosphate (MDP), offers an effective cementing of restorations even when limited retention surface is available (8-10). However, there is still controversy about APA`s potential threat to Y-TZP`s longevity, i.e., strength degradation and premature failures, given its invasive, subtractive nature of brittle ceramic surface roughening introducing surface cracks and plastic deformation (11, 12).

In light of these facts, there is still big impetus for developing a new, simple approach to improve adhesion to Y-TZP surface in a non-invasive manner, which would further have an essential role in establishing a long-term success of a Y-TZP restorations, especially when bonding surface is

limited (2). Several surface pretreatment methods have been already proposed and evaluated (13-24). However, these methods are rather complicated, time-consuming or expensive and as such not implementable in everyday dental laboratory practice. Also, only limited evidence of bond durability has been found (25).

Alternative non-invasive pretreatment to enhance the resin-Y-TZP bond, not promoting any surface flaws nor stresses that could impair the strength of the ceramics has recently been proposed by Jevnikar et al. (26) It relies on functionalization of the Y-TZP surface with a nano-structured (hydrous) alumina coating (NAC). The application of the coating provides an additive nano-roughening of the ceramic surface resulting in a substantial increase of surface area (27) that is available for bonding. It was indeed shown that NAC offers a much stronger and more durable resin-Y-TZP bond than conventional APA surface pretreatment due to the increased affinity of the functionalized Y-TZP surface for wetting and mechanical interlocking of the resin as well as the glass ionomer cements (26, 28). The original application of alumina coating was based on the precipitation of aluminium oxyhydroxide, boehmite (γ-AlOOH) by exploiting the hydrolysis of aluminium nitride (AlN) powder suspension (29). The synthesis method was later refined to be suitable for a simple, everyday dental laboratory practice, that is, starting from a clear, aluminate-based solution (VALLBOND, Vall-cer, Ljubljana, Slovenija) instead of hydrolysing AlN powder suspension, albeit providing an analogous nanostructured boehmite coating. The boehmite coating is converted to transient aluminas upon calcination the topotactic transformation (30) resulting in no change in the morphology. The effect of NAC on resin-Y-TZP bond strength was studied with calcination of deposited coating set at 900 °C for 1 hour (26, 28), transforming it to δ-Al_2O_3 (31). However, such a long thermal treatment protocol is not suitable for routine work at the dental laboratory.

To overcome this problem and effectively implement the alumina coating into routine manufacturing of Y-TZP restorations, it is necessary to combine the coating's calcination heating strategy with those encountered in dental laboratory procedures, which can, in turn, affect both the NAC chemical composition and the resin-Y-TZP bond. Thus, this work aimed at studying the effect of

various firing procedures, such as glaze, veneer and Y-TZP regeneration firing on the phase evolution of freshly deposited boehmite coating, ultimately affecting the bond between resin cement and coated Y-TZP ceramics.

2. Materials and methods

2.1 Specimens preparation

Y-TZP ceramic substrates were fabricated from commercially available, ready-to-press biomedical-grade TZ-3YB-E zirconia granulated powder (Tosoh, Tokyo, Japan), containing 3 mol.% of yttria in the solid solution to stabilize the tetragonal structure, 0.25 wt.% of alumina to lower the affinity towards the t→m transformation during ageing, and 3 wt.% of an organic binder. This material is most commonly used in the fabrication of biscuit-sintered zirconia blanks. Green pellets 20 mm in diameter and 3.5 mm in thickness were shaped with a uni-axial dry pressing at 150 MPa in a floating-head die. They were then pressure-less sintered at 1520 ◦C for 2 h. After firing, 120 disc-shaped specimens (15.5 ± 0.03 mm in diameter and 2.6 ± 0.03 mm thick) were produced and randomly divided into eight groups of 20 and subjected to the following pretreatment conditions:

Group 1: Left as-sintered to serve as a control (AS).

Group 2: high-pressure abraded with 110-micron-sized fused aluminium oxide particles at four bars for 15 s (APA-110).

Group 3: low-pressure abraded with 50-micron-sized fused aluminium oxide particles at 1 bar for 15 s (APA-50).

Group 4: low-pressure abraded with 50-micron-sized fused aluminium oxide particles at 1 bar for 15 s. Subsequently primer containing MDP monomer (Monobond Plus, Ivoclar, Lichenstein) was applied to zirconia surface (APA-50M).

During the air abrasion procedure discs were mounted in a specimen holder at a distance of 10 mm from the tip of the air-abrasion unit, equipped with a nozzle 5 mm in diameter. All the specimens were ultrasonically cleaned in acetone, ethanol and deionised water for 2 min in each solvent.

Groups 5-8: coated with NAC.

The VALLBOND precursor solution, a commercially available synthesis precursor for dental laboratories, was used for the synthesis of alumina coating. It is a clear, supersaturated aluminate solution, which upon heating up to the boiling point results in the condensation of polynuclear

aluminium species followed by heterogeneous precipitation of the boehmite (32), forming a nanostructured (hydrous) aluminium oxide coating onto the immersed substrates. Specimens were cleaned with pressurised water steam for 10 s. A batch of 10 specimens was inserted into a glass beaker containing 100 ml clear, aluminate-based precursor solution. The solution containing specimens was brought to boiling in approximately 5 minutes by using magnetic laboratory agitator with a hot plate. After 10 minutes of boiling the solution became turbid, which indicated that the synthesis of the nanostructured boehmite coating on the surface of the specimens was completed. The coated specimens were rinsed with deionised water and oven dried for 2 h at 110 °C prior to calcination at given thermal treatment conditions.

The calcination was performed in an electric resistance furnace in atmospheric air at different thermal treatment conditions, simulating firing protocols used for various laboratory procedures involved in Y-TZP restoration fabrication summarised in Table 1, varying the final firing temperature and holding time. The heating rate for all the firing protocols was set at 40 °C/min.

2.2. Coating morphology and evolution assessment

The coating morphology was assessed by scanning electron microscopy (SEM; JSM-7600F, Jeol, Japan) using accelerating voltage of 5 kV. Before it, the inspected surfaces were carbon coated. To analyse the cross-sections of the NAC-coated Y-TZP disks after thermal treatment, representative samples were fractured and analysed using SEM.

The crystal structure of the NAC deposited on Y-TZP as-sintered surfaces after synthesis, and different thermal treatment conditions were analysed in situ using grazing incidence (GI) X-ray diffraction (XRD) using a PANalytical Empyrean diffractometer equipped with the *in situ* heating stage with Cu Kα radiation (λ = 1.54187 Å) at 45 kV and 40 mA. A divergence slit with a 0.03125° fixed angle and an anti-scatter slit with a 0.0625° fixed angle were used on the incident beam side, while a parallel plate collimator with a 0.27° opening, a ß-filter (Ni foil), and 0.04 rad soller slits was used on the diffracted beam side. The GI angle (ω) was fixed at 0.67° to maximise the signal from the coating.

The X-ray patterns were obtained in the 2θ range from 43.5° to 48° with a step size of 0.024° immediately after the sample was heated and dwelled to a desired temperature and time, respectively at a heating rate of 40 °C/min. Since the as-synthesized coating did not provide any noticeable diffraction peaks on XRD in the preliminary recordings, the synthesis of the coating by using Vallbond precursor was repeated for 20-times on the same Y-TZP disks, which provided thick enough coating yielding clear diffraction peaks.

2.3 Shear bond strength testing

2.3.1. Quantitative assessment

Composite resin cylinders were fabricated by filling a modified Teflon mould with an inner diameter of 4 mm and height of 3 mm with a composite resin Filtec Z250 (3M ESPE, St. Paul, USA) in two increments. Each increment was light polymerised for 20 s with a light source (Elipar II, 3M ESPE, St. Paul, USA) positioned immediately above the specimen. The composite cylinder was then removed from a Teflon mould and additionally light cured for 20 s. Composite cylinders were bonded to Groups 1-8 with a self-adhesive bis-GMA/TEGDMA based resin cement Rely X Unicem containing phosphate adhesive monomer (3M ESPE, St. Paul, USA). The specimens were positioned in a custom-made alignment apparatus to standardise the bonding procedure and to ensure that the cylinder axis was perpendicular to the specimen surface. A weight of 750 g was added to the alignment apparatus during bonding (33). Excess cement was removed with disposable microbrushes, and the resin cement was polymerised for 40 s radially along the ceramic-composite cylinder interface. The bonded specimens were then left for 10 min at room temperature. Each surface-treated Y-TZP ceramic group was divided into two subgroups of 10 each and either stored in distilled water at 37 °C for 24 h or thermally cycled (TC). The latter were subjected to 12,000 cycles between 5 and 55 °C with a dwell time of 15 s (Thermocycler THE 1200C, SD Mechatronic, Feldkirchen-Westerham, Germany). Shear bond strength was tested with a universal testing instrument (Instron 4301, Instron Corp., Norwood, USA). A shear load was applied at the base of the resin cement at a 1 mm/min

crosshead speed until failure. The shear bond strengths (SBS) were expressed in MPa (N/m^2) and calculated using the following equation:

$$\sigma_{shear} = F/A, \quad [1]$$

where *F* is the stress load at failure (N), and *A* is the adhesive area.

2.3.2. Qualitative assessment

SEM at accelerating voltage of 5 kV was used to examine debonded ceramic surfaces of the thermocycled specimens and to assess the mode of failure. The percentage of the bonding area covered with residual NAC was assessed by calculating the coated area/bonding area pixel ratio. This analysis was performed using Photoshop CS4 software package (Adobe Systems, San Jose, USA).

Shapiro-Wilk and Levene tests were performed to assess the assumptions of normality of the data and homogeneity of variances. For each surface pretreatment condition, t-tests of independent samples assuming unequal variances were performed to assess the SBS differences between the respective non-cycled and cycled subgroups. The p-values were adjusted using the Bonferroni correction method for the multiple comparisons.

The SBS data were then split according to storage condition, and one-way ANOVA with Welch statistic (surface pretreatment as an independent factor) and Games-Howell post hoc test assuming unequal variances were carried out to assess the SBS differences for each storage condition separately. *P* values below 0.05 were considered statistically significant. The statistical analysis was performed using SPSS software, version 20 (IBM, New York, USA).

3. Results

3.1. Coating morphology and evolution evaluation

The alumina coating was deposited on the clean, as-sintered Y-TZP surface without any pretreatment. It consists of numerous, interconnected lamellar-like 2D nanosheets (Fig. 1a) that are homogeneously distributed throughout the entire Y-TZP surface area covering the surface grains of the Y-TZP, as visible from the lower magnification image (Fig. 1b). Also visible in Fig. 1b are several-micron-sized globular particles of aggregated 2D nanosheets that have homogeneously precipitated during synthesis and attached to the surface (inset of Fig. 1b). Presumably these precipitates are responsible for making the aluminate solution turbid. The thickness of the deposited coating is in the range of 0.5–0.7 microns, as presented in Fig. 1c. The coating gets denser near the Y-TZP surface, being coherently adhered to the ceramic surface with no voids or signs of delamination. In contact with the coating, several grains about 300 nm in size are clearly discernible from the fractured cross-section of the coated Y-TZP specimen.

The phase composition of the freshly deposited alumina coating was determined by using grazing incidence (GI) XRD. From the XRD pattern shown in Fig. 2a it can be seen that the coating consists solely from the Boehmite phase, an aluminium oxyhydroxide (γ-AlOOH), as according to the JCPDS data (File card No. 74-1895). Small peaks of Y-TZP surface are also visible. To analyse phase evolution during thermal treatment conditions simulating different firing protocols used for Y-TZP restoration fabrication in the dental laboratory, the specimens were additionally recorded after thermal treatment of the coating in 43.5-48° 2Θ range, which is the most suitable range where various transition aluminas can be differentiated. The diffractograms are shown in Fig. 2b. After thermal treatment at 725 °C for 1 minute at a heating rate of 40 °C/min, the Boehmite was transformed to transition γ-Al_2O_3 form (JCPDS card No. 10-425). γ-Al_2O_3 form of the coating persisted even after increasing the temperature to 900 °C and prolonging the dwell time to 30 minutes (Fig. 2b). However, thermal treatment at 1050°C for 15 minutes resulted in the topotactical transformation of γ- leading to most probably a mixture of both δ- and θ-Al_2O_3. This is indicative by the slight splitting of

the 45.75° 2θ peak to the pronounced, lower-2-theta one at 45.20° and two weak, higher-2-theta ones at about 46.50° and 47.50° corresponding to δ- (JCPDS card No. 4-877) and θ-Al_2O_3 (JCPDS card No. 11-517) phases, respectively. The phase transformation to δ-/θ-Al_2O_3 was also accompanied by slight morphological change as seen from Fig. 2c. The nanosheets consisting the coating have become thicker and shallower on the account of sintering or consolidation (34, 35) as a result of the disappearance of the mesoporosity typical for the γ-phase (36). No α-Al_2O_3, however, which is the most thermodynamically stable alumina, was observed at these thermal treatment conditions.

3.2. Shear bond strength

Means, standard deviations and statistical differences between the SBS values of all tested groups are shown in Figure 3. To quantitatively evaluate the bonding potential of NAC calcinated under different thermal treatment conditions, SBS values of AS, air abraded groups APA-110, APA-50, APA-50M and coated groups C-725(1min), C-900(1min), C-900(30min), C-1050(15min) were compared. TC was used to simulate intraoral ageing conditions. Both Y-TZP surface pretreatment and storage had a significant effect on SBS (P<0,05). The SBS increased with temperature and firing time of the simulated firing protocols used for Y-TZP restoration fabrication in the dental laboratory. There was no increase in SBS when increasing firing temperature from 900 to 1050 °C, although SBS increased with the prolongation of the holding firing time.

After TC AS group exhibited spontaneous debonding in a complete adhesive failure mode and was therefore not evaluated by SEM. Representative lower and higher magnification SEM micrographs of the fracture interfaces after SBS testing are shown in Fig. 4a-f. In low-pressure abraded group APA-50 (Fig. 4a) a complete adhesive failure occurred with no cement residues remaining on the abraded surface (inset of Fig. 4a). In all the other examined groups mixed failure mode occurred with small areas of resin cement residues observed on the Y-TZP surface. In the case of APA-110 specimen, the majority of the failure was adhesive (inset of Fig. 4b) with the small remnants of cement residing on the surface (Fig. 4b) exhibiting substantial plastic deformation and

sharp cuts resulting from the impacts of incoming Al_2O_3 particles. In the coated groups C-725(1min), C-900(1min), C-900(30min), C-1050(15min) (Fig. 4c-f) small remnants of cement and different amount of alumina coating residues were observed. Residues of NAC remained firmly bonded to the substrate after the fracture.

4. Discussion

In the present work the effect of various firing procedures on the phase evolution of NAC was examined and the resin-bond strength to NAC-coated Y-TZP surface depending on the firing protocol employed was characterised.

There are many different dental laboratory procedures involved in Y-TZP restoration fabrication. However, surface treatments such as polishing and glazing usually present the last step in the fabrication of both veneered or monolithic Y-TZP restorations and could be potentially coupled with the freshly deposited boehmite coating calcination heating strategy to transform it to alumina. The temperature of NAC calcination is one of the main factors influencing its performance. Therefore, NAC was studied under thermal treatment conditions which simulated veneer and glaze firing protocols for low- and high-fusing ceramics, whereas the commonly accepted borderline between the low- and high-fusing ceramics is at 800°C (37) such as for fluoronanoapatite glass-ceramics (38) and feldspathic veneering porcelain (39), represented in groups C-725(1min) and C-900(1min) respectively. Thermal treatment conditions in groups C-900(1min) and C-725(1min) also simulated glaze firing protocols of monolithic Y-TZP restoration for low- and high-melting ceramic glazes, without expecting significant variations in NAC performance due to small differences in some parameters between veneer and glaze firings.

The calcination of alumina coating in group C-1050(15min) was performed under thermal treatment conditions which simulated regenerative firing protocol of Y-TZP restoration. The so-called »regeneration firing« is recommended to reverse any stress-induced phase transitions from tetragonal to monoclinic phase that arise after corrective grinding of Y-TZP restoration, which can be employed to ensure a space for veneering material, to adjust an occlusal surface or to improve the fitting of the restoration (40).

According to grazing incidence (GI) XRD, the as-deposited alumina coating was topotactically transformed from boehmite to the transition γ-Al_2O_3 phase with no change in the morphology after only 1 minute at 725°C, represented by group C-725(1min) (Fig. 2b). For both sample groups C-900(1

min) and C-900(30min), which were thermally treated at 900°C for 1 and 30 minutes, respectively, the phase of the NAC still consisted of γ-Al_2O_3 (Fig. 2b). At 900°C powder-like boehmite is transformed to δ-Al_2O_3, however, such transformation has not yet occurred. A similar observation was made by Zhang et al., who showed with TEM that the sol-gel derived boehmite film deposited on the austenitic stainless steel transformed to γ-Al_2O_3 after thermal treatment at 900°C for 15 min (41). Under the regeneration firing protocol, i.e., 15 min at 1050°C, the transition from γ-Al_2O_3 to a mixture of δ/θ-Al_2O_3 (Fig. 2b) took place with a slight change in the morphology (Fig. 2c).

The firing protocol employed had a significant influence on the resin shear bond strength of NAC-coated Y-TZP surfaces (Fig. 3) before and after thermocycling (TC). TC was employed to investigate the durability of the resin-Y-TZP bond. It generates mechanical fatigue at the bonding interface (42, 43), which was shown to significantly decrease the bond strength in a comparable amount as long-term water storage (44).

Calcination of alumina coating under thermal treatment conditions simulating veneer or glaze firing protocol for low-fusing ceramics, represented by group C-725(1min), during which NAC was in the γ-Al_2O_3 form (Fig. 2b) resulted in significantly lower SBS values compared to the other coated groups. Calcination of alumina coating under thermal treatment conditions simulating veneer or glaze firing protocol for high-fusing ceramics, represented in group C-900(1min), when NAC was still in the γ-Al_2O_3 form (Figure 2b), significantly increased resin-Y-TZP bond strength for approximately 15 MPa. This was indicative that the calcination under higher temperature thermal treatment conditions is beneficial for the coatings` improved adhesion to Y-TZP surface resulting in higher SBS values. In contrast, when simulating Y-TZP regeneration firing protocol, evident in group C-1050(15min), where NAC was transformed to a mixture of δ/θ-Al_2O_3, the SBS values were slightly decreased, although statistically not significant, as compared to those measured at 900°C. The slight decrease in the SBS values of δ/θ-Al_2O_3 that was thermally treated at higher temperatures can be explained in the decreased mesoporosity and nanoscaled features of the δ/θ-Al_2O_3 forms as

compared to γ-Al_2O_3 [44] resulting in a lower surface area of the coating and decreased coating-resin interface corroborating to lower SBS values. TC did not affect SBS values of the coated groups.

The benefit of calcination under higher temperature thermal treatment conditions on the adhesive performance of alumina coating was further evident from the observed failure modes where only traces of coating residues (<5 % of the bonding area) and thus weaker bonds between Y-TZP substrate surface and NAC were present at 725°C, resulting in more easy coating delamination (Fig. 4c). In contrast, when calcination was performed at higher temperature thermal treatment conditions, more residual coating areas (30-67 % of the bonding area) were observed on the Y-TZP surface (Fig. 4e,f) indicating stronger bonds between Y-TZP substrate surface and NAC.

To evaluate the performance of alumina coating it was compared to a commonly used Y-TZP surface pretreatment such as air-abrasion, while as-sintered group served as a control. RelyX Unicem resin cement that contains the phosphate adhesive monomer was used since it has been shown that it effectively promotes durable bonding to high-pressure air abraded Y-TZP surface (45, 46). It has also been shown that a combination of resin cement and priming of the Y-TZP surface with MDP containing primer provide a durable bond even when the Y-TZP surface is pretreated using low-pressure air abrasion, which is less invasive regarding potentially damaging the Y-TZP restoration`s surface (47, 48). Also it has been previously shown

The initial resin-Y-TZP bond strength in the AS group was significantly lower compared to other groups (Fig. 3) since such surface did not provide a sufficient roughness for the mechanical interlocking. In addition, TC affected resin-Y-TZP bond, causing spontaneous debonding, indicating the inability of phosphate adhesive monomer present in the cement to create a stable chemical bond (47, 49). In the APA groups, air abrasion increased the Y-TZP`s surface roughness, improving the wetting (6, 46, 50), which provided higher initial bond strength as compared to AS group. TC only affected low-pressure abraded groups APA-50 and APA-50M. In the APA-50 group, three samples were spontaneously debonded, and a mean SBS of the other samples was significantly lowered. In the case when using MDP primer no spontaneous debonding occurred, although there was a

statistically significant drop in mean SBS. These findings are not in line with previous studies (47, 48) where even after TC resin-Y-TZP bond above 20 MPa was achieved, which represents a clinically acceptable and durable bond (7, 51). Although recently not recommended, high-pressure abrasion (APA-110) provided similar bond strength after TC as did the low-pressure abrasion in a combination with MDP primer. The low SBS values corroborated well with the evaluated failure modes (Fig. 4) which were of the adhesive type for low-abrasion groups APA-50 and APA-50M (Fig. 4a), whereas all the coated groups (Fig. 4c-f) and APA-110 group (Fig. 4b) exhibited mixed failure mode (Fig. 4b-f), where adhesive fracture between the cement and Y-TZP substrate surface was predominant.

Further, It has alredy been confirmed with TEM analysis that the resin cement, due to its sufficient wettability, efficiently penetrates into the nano-dimensional inter-lammelar spaces forming an intermediate structure designated as the hybrid layer (26) on which the bond strength is dependent. Accordingly, in groups C-900(30min) and C-1050(15min) where the NAC was thermally treated at higher temperatures and longer firing times (Fig. 4e and 4f) the NAC-Y-TZP bond was presumably stronger than the cohesive strength of the resin cement, thus, exhibiting more NAC residual areas and the highest SBS among the coated samples.

5. **Conclusions**

The present study showed that the application of a nanostructured alumina coating for the modification of the Y-TZP`s surface restoration production fabrication could be successfully integrated into the daily dental laboratory workflow. In addition, coupling NAC calcination treatment with high temperature firing protocols provides clinically acceptable resin-Y-TZP bond that is superior to the bond strength provided by low-pressure abrasion and MDP containing primer. This surface pretreatment, albeit commonly used, introduces surface flaws regarding cracks or particle inclusions that could potentially lead to premature failure of the Y-TZP restoration. On the contrary alumina coating offers an additive, non-invasive surface conditioning for the nanoroughening of the Y-TZP surfaces especially when limited retention form and bonding surface is available.

Acknowledgements

This work was supported by the Slovenian Research Agency through the research program P2-0087 and project J2-9222. The authors thank Urška Gabor for conducting the XRD measurements.

References

1. Manicone PF, Rossi Iommetti P, Raffaelli L. An overview of zirconia ceramics: basic properties and clinical applications. J Dent. 2007 Nov;35(11):819-26.

2. Ozcan M, Bernasconi M. Adhesion to zirconia used for dental restorations: a systematic review and meta-analysis. J Adhes Dent. 2015 Feb;17(1):7-26.

3. Blatz MB, Sadan A, Kern M. Resin-ceramic bonding: a review of the literature. J Prosthet Dent. 2003 Mar;89(3):268-74.

4. Thompson JY, Stoner BR, Piascik JR, Smith R. Adhesion/cementation to zirconia and other non-silicate ceramics: where are we now? Dent Mater. 2011 Jan;27(1):71-82.

5. Della Bona A, Anusavice KJ. Microstructure, composition, and etching topography of dental ceramics. Int J Prosthodont. 2002 Mar-Apr;15(2):159-67.

6. Kern M, Wegner SM. Bonding to zirconia ceramic: adhesion methods and their durability. Dent Mater. 1998 Jan;14(1):64-71.

7. Papia E, Larsson C, du Toit M, Vult von Steyern P. Bonding between oxide ceramics and adhesive cement systems: a systematic review. J Biomed Mater Res B Appl Biomater. 2014 Feb;102(2):395-413.

8. Abou Tara M, Eschbach S, Wolfart S, Kern M. Zirconia ceramic inlay-retained fixed dental prostheses - first clinical results with a new design. J Dent. 2011 Mar;39(3):208-11.

9. Sasse M, Eschbach S, Kern M. Randomized clinical trial on single retainer all-ceramic resin-bonded fixed partial dentures: Influence of the bonding system after up to 55 months. J Dent. 2012 Sep;40(9):783-6.

10. Sasse M, Kern M. Survival of anterior cantilevered all-ceramic resin-bonded fixed dental prostheses made from zirconia ceramic. J Dent. 2014 Jun;42(6):660-3.

11. Zhang Y, Lawn BR, Malament KA, Van Thompson P, Rekow ED. Damage accumulation and fatigue life of particle-abraded ceramics. Int J Prosthodont. 2006 Sep-Oct;19(5):442-8.

12. Wang H, Aboushelib MN, Feilzer AJ. Strength influencing variables on CAD/CAM zirconia frameworks. Dent Mater. 2008 May;24(5):633-8.

13. Atsu SS, Kilicarslan MA, Kucukesmen HC, Aka PS. Effect of zirconium-oxide ceramic surface treatments on the bond strength to adhesive resin. J Prosthet Dent. 2006 Jun;95(6):430-6.

14. Derand T, Molin M, Kvam K. Bond strength of composite luting cement to zirconia ceramic surfaces. Dent Mater. 2005 Dec;21(12):1158-62.

15. Lung CY, Kukk E, Matinlinna JP. The effect of silica-coating by sol-gel process on resin-zirconia bonding. Dent Mater J. 2013;32(1):165-72.

16. Usumez A, Hamdemirci N, Koroglu BY, Simsek I, Parlar O, Sari T. Bond strength of resin cement to zirconia ceramic with different surface treatments. Lasers Med Sci. 2013 Jan;28(1):259-66.

17. Everson P, Addison O, Palin WM, Burke FJ. Improved bonding of zirconia substructures to resin using a "glaze-on" technique. J Dent. 2012 Apr;40(4):347-51.

18. Phark JH, Duarte S, Jr., Blatz M, Sadan A. An in vitro evaluation of the long-term resin bond to a new densely sintered high-purity zirconium-oxide ceramic surface. J Prosthet Dent. 2009 Jan;101(1):29-38.

19. Egilmez F, Ergun G, Cekic-Nagas I, Vallittu PK, Ozcan M, Lassila LV. Effect of surface modification on the bond strength between zirconia and resin cement. J Prosthodont. 2013 Oct;22(7):529-36.

20. Aboushelib MN, Kleverlaan CJ, Feilzer AJ. Selective infiltration-etching technique for a strong and durable bond of resin cements to zirconia-based materials. J Prosthet Dent. 2007 Nov;98(5):379-88.

21. Akyil MS, Uzun IH, Bayindir F. Bond strength of resin cement to yttrium-stabilized tetragonal zirconia ceramic treated with air abrasion, silica coating, and laser irradiation. Photomed Laser Surg. 2010 Dec;28(6):801-8.

22. Lv P, Qu M, Jiang T. Effect of hot-etching treatment on shear bond strength of zirconia to resin cement. Advances in Applied Ceramics. 2018;118(1-2):16-22.

23. Zhang J, Hu W, Stijacic T, Chung K-H, Li T, Shen Z. Bonding of novel self-glazed zirconia dental ceramics. Advances in Applied Ceramics. 2018;118(1-2):37-45.

24. Yang X, Liu Y. Influence of different surface treatments on zirconia/resin shear bond strength using one-bottle universal adhesive. Advances in Applied Ceramics. 2018;118(1-2):70-7.

25. Kern M. Bonding to oxide ceramics-laboratory testing versus clinical outcome. Dent Mater. 2015 Jan;31(1):8-14.

26. Jevnikar P, Krnel K, Kocjan A, Funduk N, Kosmac T. The effect of nano-structured alumina coating on resin-bond strength to zirconia ceramics. Dent Mater. 2010 Jul;26(7):688-96.

27. Kocjan A, Dakskobler A, Kosmac T. Superhydrophobic Nanostructured Boehmite Coatings Prepared by AlN Powder Hydrolysis. International Journal of Applied Ceramic Technology. 2011;8(4): 848-53.

28. Jevnikar P, Golobič M, Kocjan A, Kosmač T. The effect of nano-structured alumina coating on the bond strength of resin-modified glass ionomer cements to zirconia ceramics. Journal of the European Ceramic Society. 2012;32(11):2641-5.

29. Krnel K, Kocjan A, Kosmač T. A simple method for the preparation of nanostructured aluminate coatings. J Am Ceram Soc. 2009;92:2451–4.

30. Krokidis X, Raybaud P. Theoretical study of the dehydration process of boehmite to γ-alumina. J Phys Chem B. 2001;105(22):5121-30.

31. Levin I, Brandon D. Metastable alumina polymorphs: crystal structures and transition sequences. J Am Ceram Soc 1998;81:1995-2012.

32. Jolivet J-P. Metal Oxide Chemistry and Synthesis: From Solution to Solid State: Wiley; 2000.

33. Hummel M, Kern M. Durability of the resin bond strength to the alumina ceramic Procera. Dent Mater. 2004 Jun;20(5):498-508.

34. Dakskobler A, Kocjan A, Kosmač T. Porous Alumina Ceramics Prepared by the Hydrolysis-Assisted Solidification Method. J Am Ceram Soc. 2011;94:1374-9

35. Krnel K, Kocjan A, Kosmač T. A Simple Method for the Preparation of Nanostructured Aluminate Coatings. J Am Ceram Soc. 2009;92 2451-4.

36. Euzen P, Raybaud P, Krokidi X, Toulhoat H, Loarer JLL, Jolivet JP, et al. Alumina. In: Schuth F, Sing JSW, Weitkamp J, editors. Hand Book of Porous Solids. Chichester: Wiley; 2002. p. 1591-677.

37. Leinfelder KF. Porcelain esthetics for the 21st century. J Am Dent Assoc. 2000 Jun;131 Suppl:47S-51S.

38. Ivoclar. IPS e.max CAD: Instructions for use. Schaan / Liechtenstein: Ivoclar Vivadent AG; 2009. p. 52.

39. VITA, VM9, Working, Instructions. Bad Säckingen, Germany: VITA Zahnfabrik H. Rauter GmbH & Co.KG; 2013. p. 23.

40. Guazzato M, Quach L, Albakry M, Swain MV. Influence of surface and heat treatments on the flexural strength of Y-TZP dental ceramic. J Dent. 2005 Jan;33(1):9-18.

41. Zhang X, Honkanen M, Pore V, Levänen E, Mäntylä T. Effect of heat treating gel films on the formation of superhydrophobic boehmite flaky structures on austenitic stainless steel. Ceram Int 2009;35:1559-64.

42. Heikkinen TT, Matinlinna JP, Vallittu PK, Lassila LV. Long term water storage deteriorates bonding of composite resin to alumina and zirconia short communication. Open Dent J. 2013;7:123-5.

43. Gale MS, Darvell BW. Thermal cycling procedures for laboratory testing of dental restorations. J Dent. 1999 Feb;27(2):89-99.

44. Santerre JP, Shajii L, Leung BW. Relation of dental composite formulations to their degradation and the release of hydrolyzed polymeric-resin-derived products. Crit Rev Oral Biol Med. 2001;12(2):136-51.

45. Mirmohammadi H, Aboushelib MN, Salameh Z, Feilzer AJ, Kleverlaan CJ. Innovations in bonding to zirconia based ceramics: Part III. Phosphate monomer resin cements. Dent Mater. 2010 Aug;26(8):786-92.

46. Luthy H, Loeffel O, Hammerle CH. Effect of thermocycling on bond strength of luting cements to zirconia ceramic. Dent Mater. 2006 Feb;22(2):195-200.

47. Yang B, Barloi A, Kern M. Influence of air-abrasion on zirconia ceramic bonding using an adhesive composite resin. Dent Mater. 2010 Jan;26(1):44-50.

48. Kern M, Barloi A, Yang B. Surface conditioning influences zirconia ceramic bonding. J Dent Res. 2009 Sep;88(9):817-22.

49. de Souza GM, Silva NR, Paulillo LA, De Goes MF, Rekow ED, Thompson VP. Bond strength to high-crystalline content zirconia after different surface treatments. J Biomed Mater Res B Appl Biomater. 2010 May;93(2):318-23.

50. Hallmann L, Ulmer P, Lehmann F, Wille S, Polonskyi O, Johannes M, et al. Effect of surface modifications on the bond strength of zirconia ceramic with resin cement resin. Dent Mater. 2016 May;32(5):631-9.

51. Lambrechts P, Inokoshi S, Van Meerbeek B, Willems G, Braem M, Van Herle G. Classification and potential of composite luting materials. In: Mörmann WH, editor. Proceedings of the International Symposium on Computer Restorations: The state of the art of the Cerec method; Berlin: Quintessence; 1991. p. 61-90.

Figures

Fig. 1. SEM micrographs of NAC deposited on the as-sintered Y-TZP surface: (a) coatings` topography; (b) at magnification 2000x (arrows) and 20000x several homogeneously precipitated micron-sized globular particles of aggregated 2D nanosheets are evident; (c) cross-sectionioal view (1 – NAC coating; 2 – Y-TZP substrate with clearly visible Y-TZP grains).

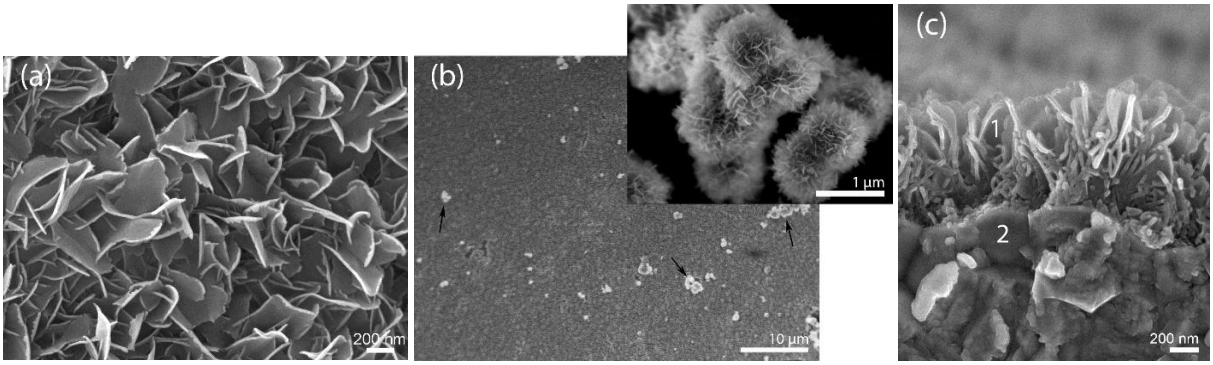

Fig. 2. Grazing incidence XRD diffractograms of the (a) boehmite phase before calcination and (b) difractograms evolved during *in situ* heating stage representing transient alumina phase evolution depending on the thermal treatment conditions; (c) Slight morphological change accompanying phase transformation to δ-/θ-Al_2O_3.

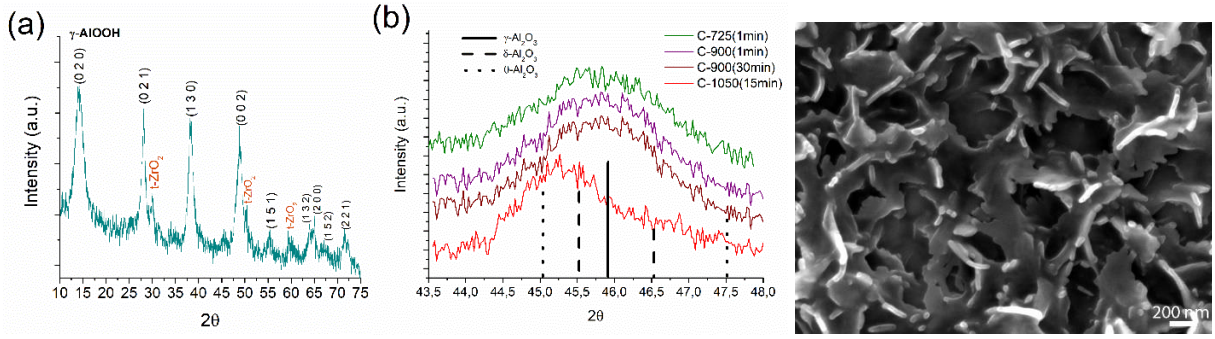

Fig. 3. Shear bond strength (SBS) means and standard deviations (SD) in Mpa of resin cement RelyX Unicem on Y-TZP ceramic after different surface pretreatment methods. SBS values marked with the same letters in the same colored bar do not differ significantly from each other.

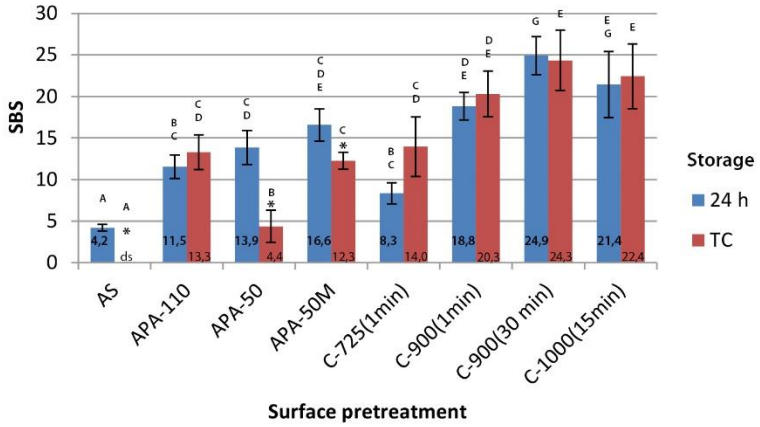

* Statistically significant (P<0.05) difference between the SBS values of the non-cycled and thermocycled subgroups of the same pretreatment group.
ds – debonded spontaneously.

Fig. 4. SEM microographs of a representative specimen from: (a) APA-50 group at 27x and 5000x magnification; (b) APA-110 group at 27x and 5000x magnification; (c) C-725(1min) group – at magnification 25x almost no NAC residues (<5 % of the bonding area) and at magnification 20000x Y-TZP grains and smaller NAC residues are evident; (d) C-900(1min) group – at magnification 25x small areas (6 % of the bonding area) of NAC residues (arrows) and at magnification 20000x Y-TZP grains and NAC residues are evident; (e) C-900(30min) group – at magnification 25x larger areas (30 % of the bonding area) of NAC residues (arrows) and at magnification 20000x Y-TZP grains and NAC residues are evident; (f) C-1050(15min) group – at magnification 25x more than half of the bonding area is covered with NAC residues (67 % of the bonding area), at magnification 20000x Y-TZP grains and NAC residues are evident. White arrow in all the figure insets labells the debonding force direction.

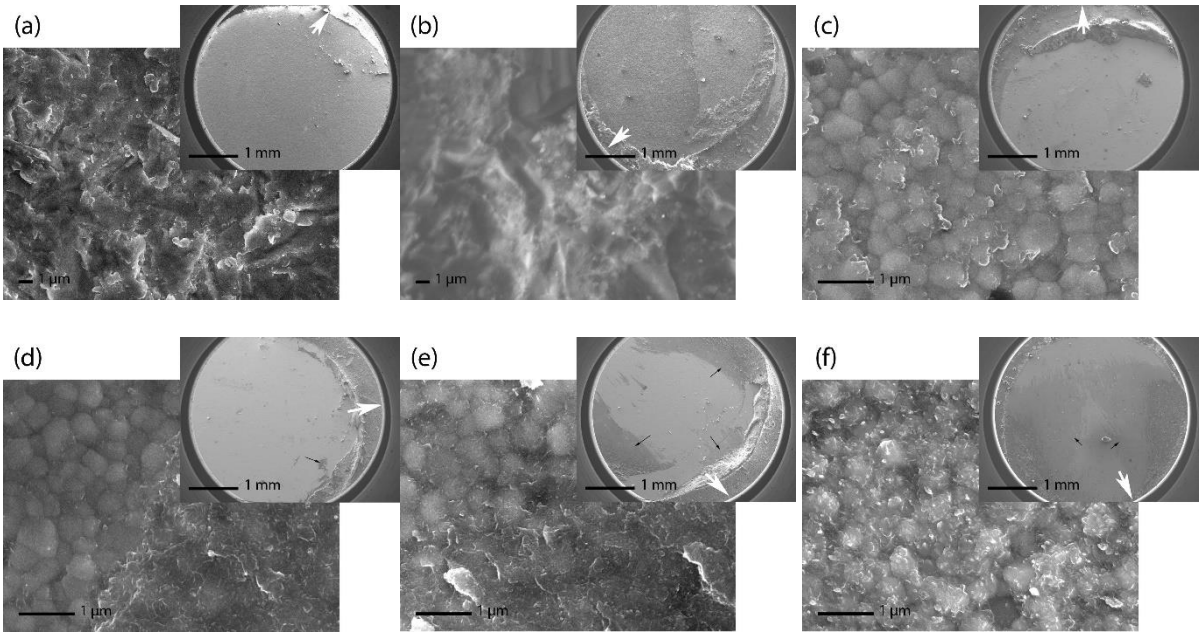

Tables

Firing protocol		*End temperature (°C)*	*Holding time (min)*
C-725(1min)	Simulating glaze or incisal veneer firing protocol for low-fusing ceramics	725	1
C-900(1min)	Simulating glaze or incisal veneer firing protocol for high-fusing ceramics	900	1
C-900(30min)	Referential thermal treatment conditions according to the manufacturer	900	30
C-1050(15min)	Simulating regeneration firing of a Y-TZP restoration(39)(39)(39)	1050	15

Table 1. Simulated firing protocols for calcination of applied NAC.